

Evidence for a bottom baryon resonance Λ_b^{*0} in CDF data

T. Aaltonen,²¹ S. Amerio,^{39b,39a} D. Amidei,³¹ A. Anastassov,^{15,w} A. Annovi,¹⁷ J. Antos,¹² G. Apollinari,¹⁵ J. A. Appel,¹⁵ T. Arisawa,⁵² A. Artikov,¹³ J. Asaadi,⁴⁷ W. Ashmanskas,¹⁵ B. Auerbach,² A. Aurisano,⁴⁷ F. Azfar,³⁸ W. Badgett,¹⁵ T. Bae,²⁵ A. Barbaro-Galtieri,²⁶ V. E. Barnes,⁴³ B. A. Barnett,²³ J. Guimaraes da Costa,²⁰ P. Barria,^{41c,41a} P. Bartos,¹² M. Bauce,^{39b,39a} F. Bedeschi,^{41a} S. Behari,¹⁵ G. Bellettini,^{41b,41a} J. Bellinger,⁵⁴ D. Benjamin,¹⁴ A. Beretvas,¹⁵ A. Bhatti,⁴⁵ K. R. Bland,⁵ B. Blumenfeld,²³ A. Bocci,¹⁴ A. Bodek,⁴⁴ D. Bortoletto,⁴³ J. Boudreau,⁴² A. Boveia,¹¹ L. Brigliadori,^{6b,6a} C. Bromberg,³² E. Brucken,²¹ J. Budagov,¹³ H. S. Budd,⁴⁴ K. Burkett,¹⁵ G. Busetto,^{39b,39a} P. Bussey,¹⁹ P. Butti,^{41b,41a} A. Buzatu,¹⁹ A. Calamba,¹⁰ S. Camarda,⁴ M. Campanelli,²⁸ F. Canelli,^{11,dd} B. Carls,²² D. Carlsmith,⁵⁴ R. Carosi,^{41a} S. Carrillo,^{16,m} B. Casal,^{9,k} M. Casarsa,^{48a} A. Castro,^{6b,6a} P. Catastini,²⁰ D. Cauz,^{48b,48c,48a} V. Cavaliere,²² M. Cavalli-Sforza,⁴ A. Cerri,^{26,f} L. Cerrito,^{28,r} Y. C. Chen,¹ M. Chertok,⁷ G. Chiarelli,^{41a} G. Chlachidze,¹⁵ K. Cho,²⁵ D. Chokheli,¹³ A. Clark,¹⁸ C. Clarke,⁵³ M. E. Convery,¹⁵ J. Conway,⁷ M. Corbo,^{15,z} M. Cordelli,¹⁷ C. A. Cox,⁷ D. J. Cox,⁷ M. Cremonesi,^{41a} D. Cruz,⁴⁷ J. Cuevas,^{9,y} R. Culbertson,¹⁵ N. d'Ascenzo,^{15,v} M. Datta,^{15,gg} P. de Barbaro,⁴⁴ L. Demortier,⁴⁵ M. Deninno,^{6a} M. D'Errico,^{39b,39a} F. Devoto,²¹ A. Di Canto,^{41b,41a} B. Di Ruzza,^{15,q} J. R. Dittmann,⁵ S. Donati,^{41b,41a} M. D'Onofrio,²⁷ M. Dorigo,^{48d,48a} A. Driutti,^{48b,48c,48a} K. Ebina,⁵² R. Edgar,³¹ A. Elagin,⁴⁷ R. Erbacher,⁷ S. Errede,²² B. Esham,²² S. Farrington,³⁸ J. P. Fernández Ramos,²⁹ R. Field,¹⁶ G. Flanagan,^{15,t} R. Forrest,⁷ M. Franklin,²⁰ J. C. Freeman,¹⁵ H. Frisch,¹¹ Y. Funakoshi,⁵² C. Galloni,^{41b,41a} A. F. Garfinkel,⁴³ P. Garosi,^{41c,41a} H. Gerberich,²² E. Gerchtein,¹⁵ S. Giagu,^{46a} V. Giakoumopoulou,³ K. Gibson,⁴² C. M. Ginsburg,¹⁵ N. Giokaris,³ P. Giromini,¹⁷ G. Giurgiu,²³ V. Glagolev,¹³ D. Glenzinski,¹⁵ M. Gold,³⁴ D. Goldin,⁴⁷ A. Golossanov,¹⁵ G. Gomez,⁹ G. Gomez-Ceballos,³⁰ M. Goncharov,³⁰ O. González López,²⁹ I. Gorelov,³⁴ A. T. Goshaw,¹⁴ K. Goulianos,⁴⁵ E. Gramellini,^{6a} S. Grinstein,⁴ C. Grosso-Pilcher,¹¹ R. C. Group,^{51,15} S. R. Hahn,¹⁵ J. Y. Han,⁴⁴ F. Happacher,¹⁷ K. Hara,⁴⁹ M. Hare,⁵⁰ R. F. Harr,⁵³ T. Harrington-Taber,^{15,n} K. Hatakeyama,⁵ C. Hays,³⁸ J. Heinrich,⁴⁰ M. Herndon,⁵⁴ A. Hocker,¹⁵ Z. Hong,⁴⁷ W. Hopkins,^{15,g} S. Hou,¹ R. E. Hughes,³⁵ U. Husemann,⁵⁵ M. Hussein,^{32,bb} J. Huston,³² G. Introzzi,^{41e,41f,41a} M. Iori,^{46b,46a} A. Ivanov,^{7,p} E. James,¹⁵ D. Jang,¹⁰ B. Jayatilaka,¹⁵ E. J. Jeon,²⁵ S. Jindariani,¹⁵ M. Jones,⁴³ K. K. Joo,²⁵ S. Y. Jun,¹⁰ T. R. Junk,¹⁵ M. Kambeitz,²⁴ T. Kamon,^{25,47} P. E. Karchin,⁵³ A. Kasmai,⁵ Y. Kato,^{37,o} W. Ketchum,^{11,hh} J. Keung,⁴⁰ B. Kilminster,^{15,dd} D. H. Kim,²⁵ H. S. Kim,²⁵ J. E. Kim,²⁵ M. J. Kim,¹⁷ S. H. Kim,⁴⁹ S. B. Kim,²⁵ Y. J. Kim,²⁵ Y. K. Kim,¹¹ N. Kimura,⁵² M. Kirby,¹⁵ K. Knoepfel,¹⁵ K. Kondo,^{52,a} D. J. Kong,²⁵ J. Konigsberg,¹⁶ A. V. Kotwal,¹⁴ M. Kreps,²⁴ J. Kroll,⁴⁰ M. Kruse,¹⁴ T. Kuhr,²⁴ M. Kurata,⁴⁹ A. T. Laasanen,⁴³ S. Lammel,¹⁵ M. Lancaster,²⁸ K. Lannon,^{35,x} G. Latino,^{41c,41a} H. S. Lee,²⁵ J. S. Lee,²⁵ S. Leo,^{41a} S. Leone,^{41a} J. D. Lewis,¹⁵ A. Limosani,^{14,s} E. Lipeles,⁴⁰ A. Lister,^{18,b} H. Liu,⁵¹ Q. Liu,⁴³ T. Liu,¹⁵ S. Lockwitz,⁵⁵ A. Loginov,⁵⁵ D. Lucchesi,^{39b,39a} A. Lucà,¹⁷ J. Lueck,²⁴ P. Lujan,²⁶ P. Lukens,¹⁵ G. Lungu,⁴⁵ J. Lys,²⁶ R. Lysak,^{12,e} R. Madrak,¹⁵ P. Maestro,^{41c,41a} S. Malik,⁴⁵ G. Manca,^{27,c} A. Manousakis-Katsikakis,³ L. Marchese,^{6a,ii} F. Margaroli,^{46a} P. Marino,^{41d,41a} M. Martínez,⁴ K. Matera,²² M. E. Mattson,⁵³ A. Mazzacane,¹⁵ P. Mazzanti,^{6a} R. McNulty,^{27,j} A. Mehta,²⁷ P. Mehtala,²¹ C. Mesropian,⁴⁵ T. Miao,¹⁵ D. Mietlicki,³¹ A. Mitra,¹ H. Miyake,⁴⁹ S. Moed,¹⁵ N. Moggi,^{6a} C. S. Moon,^{15,z} R. Moore,^{15,ee,ff} M. J. Morello,^{41d,41a} A. Mukherjee,¹⁵ Th. Muller,²⁴ P. Murat,¹⁵ M. Mussini,^{6b,6a} J. Nachtman,^{15,n} Y. Nagai,⁴⁹ J. Naganoma,⁵² I. Nakano,³⁶ A. Napier,⁵⁰ J. Nett,⁴⁷ C. Neu,⁵¹ T. Nigmanov,⁴² L. Nodulman,² S. Y. Noh,²⁵ O. Norriella,²² L. Oakes,³⁸ S. H. Oh,¹⁴ Y. D. Oh,²⁵ I. Oksuzian,⁵¹ T. Okusawa,³⁷ R. Orava,²¹ L. Ortolan,⁴ C. Pagliarone,^{48a} E. Palencia,^{9,f} P. Palni,³⁴ V. Papadimitriou,¹⁵ W. Parker,⁵⁴ G. Pauletta,^{48b,48c,48a} M. Paulini,¹⁰ C. Paus,³⁰ T. J. Phillips,¹⁴ G. Piacentino,^{41a} E. Pianori,⁴⁰ J. Pilot,⁷ K. Pitts,²² C. Plager,⁸ L. Pondrom,⁵⁴ S. Poprocki,^{15,g} K. Potamianos,²⁶ A. Pranko,²⁶ F. Prokoshin,^{13,aa} F. Ptohos,^{17,h} G. Punzi,^{41b,41a} N. Ranjan,⁴³ I. Redondo Fernández,²⁹ P. Renton,³⁸ M. Rescigno,^{46a} F. Rimondi,^{6a,a} L. Ristori,^{41a,15} A. Robson,¹⁹ T. Rodriguez,⁴⁰ S. Rolli,^{50,i} M. Ronzani,^{41b,41a} R. Roser,¹⁵ J. L. Rosner,¹¹ F. Ruffini,^{41c,41a} A. Ruiz,⁹ J. Russ,¹⁰ V. Rusu,¹⁵ W. K. Sakumoto,⁴⁴ Y. Sakurai,⁵² L. Santi,^{48b,48c,48a} K. Sato,⁴⁹ V. Saveliev,^{15,v} A. Savoy-Navarro,^{15,z} P. Schlabach,¹⁵ E. E. Schmidt,¹⁵ T. Schwarz,³¹ L. Scodellaro,⁹ F. Scuri,^{41a} S. Seidel,³⁴ Y. Seiya,³⁷ A. Semenov,¹³ F. Sforza,^{41b,41a} S. Z. Shalhout,⁷ T. Shears,²⁷ P. F. Shepard,⁴² M. Shimojima,^{49,u} M. Shochet,¹¹ A. Simonenko,¹³ K. Sliwa,⁵⁰ J. R. Smith,⁷ F. D. Snider,¹⁵ H. Song,⁴² V. Sorin,⁴ R. St. Denis,¹⁹ M. Stancari,¹⁵ D. Stentz,^{15,w} J. Strologas,³⁴ Y. Sudo,⁴⁹ A. Sukhanov,¹⁵ I. Suslov,¹³ K. Takemasa,⁴⁹ Y. Takeuchi,⁴⁹ J. Tang,¹¹ M. Tecchio,³¹ I. Shreyber-Tecker,³³ P. K. Teng,¹ J. Thom,^{15,g} E. Thomson,⁴⁰ V. Thukral,⁴⁷ D. Toback,⁴⁷ S. Tokar,¹² K. Tollefson,³² T. Tomura,⁴⁹ D. Tonelli,^{15,f} S. Torre,¹⁷ D. Torretta,¹⁵ P. Totaro,^{39a} M. Trovato,^{41d,41a} F. Ukegawa,⁴⁹ S. Uozumi,²⁵ F. Vázquez,^{16,m} G. Velev,¹⁵ C. Vellidis,¹⁵ C. Vernieri,^{41d,41a} M. Vidal,⁴³ R. Vilar,⁹ J. Vizán,^{9,cc} M. Vogel,³⁴ G. Volpi,¹⁷ P. Wagner,⁴⁰ R. Wallny,^{15,k} S. M. Wang,¹ D. Waters,²⁸ W. C. Wester III,¹⁵ D. Whiteson,^{40,d} A. B. Wicklund,² S. Wilbur,⁷ H. H. Williams,⁴⁰ J. S. Wilson,³¹ P. Wilson,¹⁵ B. L. Winer,³⁵ P. Wittich,^{15,g} S. Wolbers,¹⁵ H. Wolfe,³⁵ T. Wright,³¹ X. Wu,¹⁸ Z. Wu,⁵ K. Yamamoto,³⁷ D. Yamato,³⁷ T. Yang,¹⁵ U. K. Yang,²⁵ Y. C. Yang,²⁵ W.-M. Yao,²⁶ G. P. Yeh,¹⁵ K. Yi,^{15,n} J. Yoh,¹⁵ K. Yorita,⁵² T. Yoshida,^{37,l} G. B. Yu,¹⁴ I. Yu,²⁵ A. M. Zanetti,^{48a} Y. Zeng,¹⁴ C. Zhou,¹⁴ and S. Zucchelli^{6b,6a}

(CDF Collaboration)

- ¹*Institute of Physics, Academia Sinica, Taipei, Taiwan 11529, Republic of China*
²*Argonne National Laboratory, Argonne, Illinois 60439, USA*
³*University of Athens, 157 71 Athens, Greece*
⁴*Institut de Fisica d'Altes Energies, ICREA, Universitat Autònoma de Barcelona, E-08193 Bellaterra (Barcelona), Spain*
⁵*Baylor University, Waco, Texas 76798, USA*
^{6a}*Istituto Nazionale di Fisica Nucleare Bologna, I-40127 Bologna, Italy*
^{6b}*University of Bologna, I-40127 Bologna, Italy*
⁷*University of California, Davis, California 95616, USA*
⁸*University of California, Los Angeles, California 90024, USA*
⁹*Instituto de Fisica de Cantabria, CSIC-University of Cantabria, 39005 Santander, Spain*
¹⁰*Carnegie Mellon University, Pittsburgh, Pennsylvania 15213, USA*
¹¹*Enrico Fermi Institute, University of Chicago, Chicago, Illinois 60637, USA*
¹²*Comenius University, 842 48 Bratislava, Slovakia; Institute of Experimental Physics, 040 01 Kosice, Slovakia*
¹³*Joint Institute for Nuclear Research, RU-141980 Dubna, Russia*
¹⁴*Duke University, Durham, North Carolina 27708, USA*
¹⁵*Fermi National Accelerator Laboratory, Batavia, Illinois 60510, USA*
¹⁶*University of Florida, Gainesville, Florida 32611, USA*
¹⁷*Laboratori Nazionali di Frascati, Istituto Nazionale di Fisica Nucleare, I-00044 Frascati, Italy*
¹⁸*University of Geneva, CH-1211 Geneva 4, Switzerland*
¹⁹*Glasgow University, Glasgow G12 8QQ, United Kingdom*
²⁰*Harvard University, Cambridge, Massachusetts 02138, USA*
²¹*Department of Physics, Division of High Energy Physics, University of Helsinki, FIN-00014 Helsinki, Finland; Helsinki Institute of Physics, FIN-00014 Helsinki, Finland*
²²*University of Illinois, Urbana, Illinois 61801, USA*
²³*The Johns Hopkins University, Baltimore, Maryland 21218, USA*
²⁴*Institut für Experimentelle Kernphysik, Karlsruhe Institute of Technology, D-76131 Karlsruhe, Germany*
²⁵*Center for High Energy Physics: Kyungpook National University, Daegu 702-701, Korea; Seoul National University, Seoul 151-742, Korea; Sungkyunkwan University, Suwon 440-746, Korea; Korea Institute of Science and Technology Information, Daejeon 305-806, Korea; Chonnam National University, Gwangju 500-757, Korea; Chonbuk National University, Jeonju 561-756, Korea; Ewha Womans University, Seoul 120-750, Korea*
²⁶*Ernest Orlando Lawrence Berkeley National Laboratory, Berkeley, California 94720, USA*
²⁷*University of Liverpool, Liverpool L69 7ZE, United Kingdom*
²⁸*University College London, London WC1E 6BT, United Kingdom*
²⁹*Centro de Investigaciones Energeticas Medioambientales y Tecnológicas, E-28040 Madrid, Spain*
³⁰*Massachusetts Institute of Technology, Cambridge, Massachusetts 02139, USA*
³¹*University of Michigan, Ann Arbor, Michigan 48109, USA*
³²*Michigan State University, East Lansing, Michigan 48824, USA*
³³*Institution for Theoretical and Experimental Physics, ITEP, Moscow 117259, Russia*
³⁴*University of New Mexico, Albuquerque, New Mexico 87131, USA*
³⁵*The Ohio State University, Columbus, Ohio 43210, USA*
³⁶*Okayama University, Okayama 700-8530, Japan*
³⁷*Osaka City University, Osaka 558-8585, Japan*
³⁸*University of Oxford, Oxford OX1 3RH, United Kingdom*
^{39a}*Istituto Nazionale di Fisica Nucleare, Sezione di Padova, I-35131 Padova, Italy*
^{39b}*University of Padova, I-35131 Padova, Italy*
⁴⁰*University of Pennsylvania, Philadelphia, Pennsylvania 19104, USA*
^{41a}*Istituto Nazionale di Fisica Nucleare Pisa, I-56127 Pisa, Italy*
^{41b}*University of Pisa, I-56127 Pisa, Italy*
^{41c}*University of Siena, I-56127 Pisa, Italy*
^{41d}*Scuola Normale Superiore, I-56127 Pisa, Italy*
^{41e}*INFN Pavia, I-27100 Pavia, Italy*
^{41f}*University of Pavia, I-27100 Pavia, Italy*
⁴²*University of Pittsburgh, Pittsburgh, Pennsylvania 15260, USA*
⁴³*Purdue University, West Lafayette, Indiana 47907, USA*
⁴⁴*University of Rochester, Rochester, New York 14627, USA*
⁴⁵*The Rockefeller University, New York, New York 10065, USA*

^{46a}*Istituto Nazionale di Fisica Nucleare, Sezione di Roma 1, I-00185 Roma, Italy*^{46b}*Sapienza Università di Roma, I-00185 Roma, Italy*⁴⁷*Mitchell Institute for Fundamental Physics and Astronomy, Texas A&M University, College Station, Texas 77843, USA*^{48a}*Istituto Nazionale di Fisica Nucleare Trieste, I-33100 Udine, Italy*^{48b}*Gruppo Collegato di Udine, I-33100 Udine, Italy*^{48c}*University of Udine, I-33100 Udine, Italy*^{48d}*University of Trieste, I-34127 Trieste, Italy*⁴⁹*University of Tsukuba, Tsukuba, Ibaraki 305, Japan*⁵⁰*Tufts University, Medford, Massachusetts 02155, USA*⁵¹*University of Virginia, Charlottesville, Virginia 22906, USA*⁵²*Waseda University, Tokyo 169, Japan*⁵³*Wayne State University, Detroit, Michigan 48201, USA*⁵⁴*University of Wisconsin, Madison, Wisconsin 53706, USA*⁵⁵*Yale University, New Haven, Connecticut 06520, USA*

(Received 12 August 2013; published 1 October 2013)

Using data from proton-antiproton collisions at $\sqrt{s} = 1.96$ TeV recorded by the CDF II detector at the Fermilab Tevatron, evidence for the excited resonance state Λ_b^{*0} is presented in its $\Lambda_b^0 \pi^- \pi^+$ decay followed by the $\Lambda_b^0 \rightarrow \Lambda_c^+ \pi^-$ and $\Lambda_c^+ \rightarrow p K^- \pi^+$ decays. The analysis is based on a data sample corresponding to an integrated luminosity of 9.6 fb^{-1} collected by an online event selection based on charged-particle tracks displaced from the proton-antiproton interaction point. The significance of the observed signal is 3.5σ . The mass of the observed state is found to be $5919.22 \pm 0.76 \text{ MeV}/c^2$ in agreement with similar findings in proton-proton collision experiments.

DOI: [10.1103/PhysRevD.88.071101](https://doi.org/10.1103/PhysRevD.88.071101)

PACS numbers: 14.20.Mr, 13.30.Eg, 14.65.Fy

^aDeceased.^bVisitor from University of British Columbia, Vancouver, BC V6T 1Z1, Canada.^cVisitor from Istituto Nazionale di Fisica Nucleare, Sezione di Cagliari, 09042 Monserrato (Cagliari), Italy.^dVisitor from University of California Irvine, Irvine, CA 92697, USA.^eVisitor from Institute of Physics, Academy of Sciences of the Czech Republic, 182 21, Czech Republic.^fVisitor from CERN, CH-1211 Geneva, Switzerland.^gVisitor from Cornell University, Ithaca, NY 14853, USA.^hVisitor from University of Cyprus, Nicosia CY-1678, Cyprus.ⁱVisitor from Office of Science, U.S. Department of Energy, Washington, D.C. 20585, USA.^jVisitor from University College Dublin, Dublin 4, Ireland.^kVisitor from ETH, 8092 Zürich, Switzerland.^lVisitor from University of Fukui, Fukui City, Fukui Prefecture, Japan 910-0017.^mVisitor from Universidad Iberoamericana, Lomas de Santa Fe, México, C.P. 01219, Distrito Federal.ⁿVisitor from University of Iowa, Iowa City, IA 52242, USA.^oVisitor from Kinki University, Higashi-Osaka City, Japan 577-8502.^pVisitor from Kansas State University, Manhattan, KS 66506, USA.^qVisitor from Brookhaven National Laboratory, Upton, NY 11973, USA.^rVisitor from Queen Mary, University of London, London, E1 4NS, United Kingdom.^sVisitor from University of Melbourne, Victoria 3010, Australia.^tVisitor from Muons, Inc., Batavia, IL 60510, USA.^uVisitor from Nagasaki Institute of Applied Science, Nagasaki 851-0193, Japan.^vVisitor from National Research Nuclear University, Moscow 115409, Russia.^wVisitor from Northwestern University, Evanston, IL 60208, USA.^xVisitor from University of Notre Dame, Notre Dame, IN 46556, USA.^yVisitor from Universidad de Oviedo, E-33007 Oviedo, Spain.^zVisitor from CNRS-IN2P3, Paris, F-75205 France.^{aa}Visitor from Universidad Tecnica Federico Santa Maria, 110v Valparaiso, Chile.^{bb}Visitor from The University of Jordan, Amman 11942, Jordan.^{cc}Visitor from Universite catholique de Louvain, 1348 Louvain-La-Neuve, Belgium.^{dd}Visitor from University of Zürich, 8006 Zürich, Switzerland.^{ee}Visitor from Massachusetts General Hospital, Boston, MA 02114, USA.^{ff}Visitor from Harvard Medical School, Boston, MA 02114, USA.^{gg}Visitor from Hampton University, Hampton, VA 23668, USA.^{hh}Visitor from Los Alamos National Laboratory, Los Alamos, NM 87544, USA.ⁱⁱVisitor from Università degli Studi di Napoli Federico I, I-80138 Napoli, Italy.

Baryons with a heavy-quark Q are useful for probing quantum chromodynamics (QCD) in its confinement domain. Observing new heavy-quark baryon states and measuring their properties provides further experimental constraints to the phenomenology in this regime. This report provides an additional contribution to the currently small number of heavy-quark baryon observations.

In the framework of heavy-quark effective theories (HQET) [1,2], a bottom quark b and a spin-zero $[ud]$ diquark, carrying an angular momentum $L = 1$ relative to the b quark (hence named P -wave states) can form two excited states. These are named Λ_b^{*0} , with same quark content as the singlet Λ_b^0 [3] and isospin $I = 0$ but total spin and parity $J^P = \frac{1}{2}^-$ and $J^P = \frac{3}{2}^-$ [4]. These isoscalar states are the lightest P -wave states that can decay to the Λ_b^0 baryon via strong-interaction processes. The decays require the emission of a pair of low-momentum (soft) pions. Both Λ_b^{*0} [5] particles are classified as bottom-baryon resonant states. Several recent theoretical predictions of their masses are available. An approach based on a quark-potential model with the color hyperfine interaction is used in Ref. [6]. The authors in Ref. [7] use a constituent quark model incorporating the basic properties of QCD and solving exactly the three-body problem. A heavy baryon is considered in Ref. [8] as a heavy-quark and light-diquark system in the framework of the relativistic quark model based on the quasipotential approach in QCD. The spectroscopy of isoscalar heavy baryons and their excitations is studied in Ref. [9] within the framework of HQET at leading and next-to-leading orders in the combined inverse heavy-quark mass, $1/m_Q$, and inverse number of colors, $1/N_c$, expansions. The nonperturbative formalism of QCD sum rules is applied within HQET to calculate the mass spectra of the bottom baryon states [10]. Some calculations predict Λ_b^{*0} masses smaller than the hadronic decay kinematic threshold ($\approx 5900 \text{ MeV}/c^2$) allowing only radiative decays [7,10]. Other calculations predict the mass difference $M(\Lambda_b^{*0}) - M(\Lambda_b^0)$ for the $J^P = \frac{1}{2}^-$ state to be approximately in the range of $300\text{--}310 \text{ MeV}/c^2$ [6,8,9]. The mass splitting between the two states is predicted to be in the range of $10\text{--}17 \text{ MeV}/c^2$.

The first experimental studies of b -quark baryon resonant states were reported by CDF with the observation of the S -wave states $\Sigma_b^{(*)}$ in their $\Lambda_b^0 \pi^\pm$ decays [11,12]. The ground states of the charged bottom-strange Ξ_b^- baryon [13–15] and bottom doubly strange Ω_b^- [15,16] were reported by both CDF and D0, and later CDF observed the neutral bottom-strange baryon Ξ_b^0 [17]. Recently, LHCb reported precise mass measurements of the ground state Λ_b^0 , the Ξ_b^- state, and the Ω_b^- state [18]. The CMS Collaboration observed another bottom-strange state, Ξ_b^{*0} , which is interpreted as a $J^P = \frac{3}{2}^+$ resonance [19]. Most recently, two states interpreted as the two Λ_b^{*0} resonant states were observed by the LHCb Collaboration for the first time [20].

In this report, we present evidence for the production of a Λ_b^{*0} resonance state in CDF data. We search for candidate Λ_b^{*0} baryons produced in proton-antiproton collisions at $\sqrt{s} = 1.96 \text{ TeV}$ using a data sample from an integrated luminosity of 9.6 fb^{-1} collected by CDF with a specialized online event selection (trigger) that collects events enriched in fully hadronic decays of b hadrons. The Λ_b^{*0} candidates are identified in the pseudorapidity range $|\eta| < 1.0$ using their exclusive decays to Λ_b^0 baryons and two oppositely charged soft pions. The excellent performance of the CDF devices for measuring charged-particle trajectories (tracks) allows reconstructing charged particles with transverse momenta as low as $200 \text{ MeV}/c$. The result in this paper is the first to support the LHCb observation [20].

The component of the CDF II detector [21] most relevant to this analysis is the charged-particle tracking system, which operates in a uniform axial magnetic field of 1.4 T generated by a superconducting solenoidal magnet. The inner tracking system is comprised of a silicon tracker [22]. A large open-cell cylindrical drift chamber [23] completes the tracking system. The silicon tracking system measures the transverse impact parameter of tracks with respect to the primary interaction point, d_0 [24], with a resolution of $\sigma_{d_0} \approx 40 \mu\text{m}$, including an approximately $32 \mu\text{m}$ contribution from the beam size [22]. The transverse momentum resolution of the tracking system is $\sigma(p_T)/p_T^2 \approx 0.07\%$ with p_T in GeV/c [24].

This analysis relies on a three-level trigger to collect data samples enriched in multibody hadronic decays of b hadrons (displaced-track trigger). The trigger requires two charged particles in the drift chamber, each with $p_T > 2.0 \text{ GeV}/c$ [25]. The particle tracks are required to be azimuthally separated by $2^\circ < \Delta\phi < 90^\circ$ [24]. Silicon information is added and the impact parameter d_0 of each track is required to lie in the range of $0.12\text{--}1 \text{ mm}$ providing efficient discrimination of long-lived b hadrons [26]. Finally, the distance L_{xy} in the transverse plane between the collision space point (primary vertex) and the intersection point of the two tracks projected onto their total transverse momentum is required to exceed $200 \mu\text{m}$.

The mass resolution of the Λ_b^{*0} resonances is predicted with a Monte Carlo simulation that generates b quarks according to a calculation expanded at next-to-leading order in the strong coupling constant [27] and produces events containing final-state hadrons by simulating b -quark fragmentation [28]. In the simulations, the Λ_b^{*0} baryon is assigned the mass value of $5920.0 \text{ MeV}/c^2$. Decays are simulated with the EvtGen [29] program, and all b hadrons are simulated unpolarized. The generated events are passed to a Geant3-based [30] detector simulation, then to a trigger simulation, and finally the same reconstruction algorithm as used for experimental data.

The Λ_b^{*0} candidates are reconstructed in the exclusive strong-interaction decay $\Lambda_b^{*0} \rightarrow \Lambda_b^0 \pi_s^- \pi_s^+$, where the low-momentum pions π_s^\pm are produced near kinematic

threshold [31]. The Λ_b^0 baryon decays through the weak interaction to a baryon Λ_c^+ and a pion labeled as π_b^- to distinguish it from the soft pions. This is followed by the weak-interaction decay $\Lambda_c^+ \rightarrow pK^- \pi^+$. We search for a Λ_b^{*0} signal in the Q -value distribution, where $Q = m(\Lambda_b^0 \pi_s^- \pi_s^+) - m(\Lambda_b^0) - 2m_\pi$, $m(\Lambda_b^0)$ is the reconstructed $\Lambda_c^+ \pi_b^-$ mass, and m_π is the known charged-pion mass. The effect of the Λ_b^0 mass resolution is suppressed, and most of the systematic uncertainties are reduced in the mass difference. We search for narrow structures in the 6–45 MeV/ c^2 range of the Q -value spectrum motivated by the theoretical estimates [6,8,9] and the LHCb findings [20].

The analysis begins with the reconstruction of the $\Lambda_c^+ \rightarrow pK^- \pi^+$ decay space point by fitting three tracks to a common point. Standard CDF quality requirements are applied to each track, and only tracks corresponding to particles with $p_T > 400$ MeV/ c are used. No particle identification is used. All tracks are refitted using pion, kaon, and proton mass hypotheses to correct for the mass-dependent effects of multiple scattering and ionization-energy loss. The invariant mass of the Λ_c^+ candidate is required to match the known value [3] within ± 18 MeV/ c^2 . The momentum vector of the Λ_c^+ candidate is then extrapolated to intersect with a fourth track that is assumed to be a pion, to form the $\Lambda_b^0 \rightarrow \Lambda_c^+ \pi_b^-$ candidate. The Λ_b^0 reconstructed decay point (decay vertex) is subjected to a three-dimensional kinematic fit with the Λ_c^+ candidate mass constrained to its known value [3]. The probability of the Λ_b^0 vertex fit must exceed 0.01% [12]. The proton from the Λ_c^+ candidate is required to have $p_T > 2.0$ GeV/ c to ensure that the proton is consistent with having contributed to the trigger decision. The minimum requirement on $p_T(\pi_b^-)$ is determined by an optimization procedure maximizing the quantity $S_{\Lambda_b^0}/(1 + \sqrt{B})$ [32], where $S_{\Lambda_b^0}$ is the number of Λ_b^0 signal events obtained from the fit of the observed $\Lambda_c^+ \pi_b^-$ mass distribution, and B is the number of events in the sideband region of $50 < Q < 90$ MeV/ c^2 scaled to the background yield expected in the signal range $14.0 < Q < 26.0$ MeV/ c^2 . The sideband region boundaries are motivated by the signal predictions in Refs. [6,8,9]. The resulting requirement is found to be $p_T(\pi_b^-) > 1.0$ GeV/ c . The momentum criteria both for proton and π_b^- candidates favor these particles to be the two that contribute to the displaced-track trigger decision. To keep the soft pions from Λ_b^{*0} decays within the kinematic acceptance, the Λ_b^0 candidate must have $p_T(\Lambda_b^0) > 9.0$ GeV/ c . This maximizes the quantity $S_{MC}/(1 + \sqrt{B})$, where S_{MC} is the Λ_b^{*0} signal reconstructed in the simulation.

To suppress prompt backgrounds from primary interactions, the decay vertex of the long-lived Λ_b^0 candidate is required to be distinct from the primary vertex by requiring the proper decay time and its significance to be $ct(\Lambda_b^0) > 200 \mu\text{m}$ and $ct(\Lambda_b^0)/\sigma_{ct} > 6.0$, respectively. The first criterion validates the trigger condition, while the second is

fully efficient on simulated Λ_b^{*0} signal decays. We define the proper decay time as $ct(\Lambda_b^0) = L_{xy} m_{\Lambda_b^0} c / p_T$, where $m_{\Lambda_b^0}$ is the known mass of the Λ_b^0 baryon [3]. We require the Λ_c^+ vertex to be associated with a Λ_b^0 decay by requiring $ct(\Lambda_c^+) > -100 \mu\text{m}$, as derived from the quantity $L_{xy}(\Lambda_c^+)$ measured with respect to the Λ_b^0 vertex. This requirement reduces contributions from Λ_c^+ baryons directly produced in $p\bar{p}$ interactions and from random combinations of tracks that accidentally are reconstructed as Λ_c^+ candidates. To reduce combinatorial background and contributions from partially reconstructed decays, Λ_b^0 candidates are required to point towards the primary vertex by requiring the impact parameter $d_0(\Lambda_b^0)$ not to exceed $80 \mu\text{m}$. The $ct(\Lambda_c^+)$ and $d_0(\Lambda_b^0)$ criteria [12] are fully efficient for the Λ_b^{*0} signal.

Figure 1 shows the resulting prominent Λ_b^0 signal in the $\Lambda_c^+ \pi_b^-$ invariant mass distribution. The binned maximum-likelihood fit finds a signal of approximately 15 400 candidates at the expected Λ_b^0 mass, with unity signal-to-background ratio. The fit model describing the invariant mass distribution comprises the Gaussian $\Lambda_b^0 \rightarrow \Lambda_c^+ \pi_b^-$ signal overlapping a background shaped by several contributions. Random four-track combinations dominating the right sideband are modeled with an exponentially decreasing function. Coherent sources populate the left sideband and leak under the signal. These include reconstructed B mesons that pass the $\Lambda_b^0 \rightarrow \Lambda_c^+ \pi_b^-$ selection criteria, partially reconstructed Λ_b^0 decays, and fully reconstructed Λ_b^0 decays other than $\Lambda_c^+ \pi_b^-$ (e.g., $\Lambda_b^0 \rightarrow \Lambda_c^+ K^-$). Shapes representing the physical background sources are derived from Monte Carlo simulations. Their normalizations are constrained to branching ratios that are either measured (for B meson decays reconstructed within the same $\Lambda_c^+ \pi_b^-$ sample) or theoretically predicted (for Λ_b^0 decays). The discrepancy between the fit and the data at smaller masses

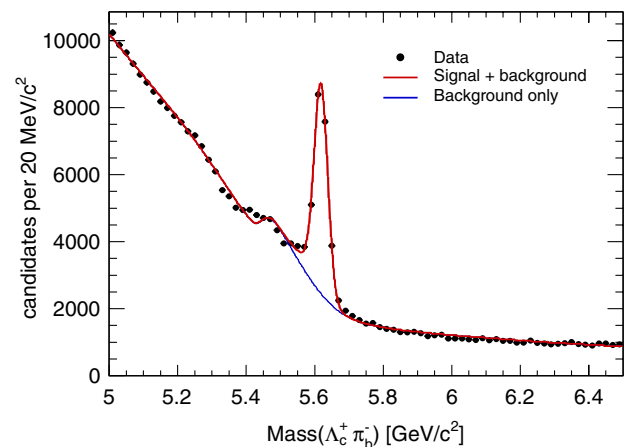


FIG. 1 (color online). Invariant mass distribution of $\Lambda_b^0 \rightarrow \Lambda_c^+ \pi_b^-$ candidates with a fit overlaid. The shoulder at the left sideband is dominated by fully reconstructed B mesons and partially reconstructed Λ_b^0 decays.

than the Λ_b^0 signal is attributed to incomplete knowledge of the branching fractions of decays populating this region [11,12,33,34] and is verified to have no effect on the final results. The fit is used only to define the Λ_b^{*0} search sample.

To reconstruct the Λ_b^{*0} candidates, each Λ_b^0 candidate with mass within the range of $5.561\text{--}5.677\text{ GeV}/c^2$ ($\pm 3\sigma$) is combined with a pair of oppositely charged particles, each assigned the pion mass. To increase the efficiency for reconstructing Λ_b^{*0} decays near the kinematic threshold, the quality criteria applied to soft-pion tracks are loosened. The basic requirements for hits in the drift chamber and main silicon tracker are imposed on the π_s^\pm tracks, and tracks reconstructed with a valid fit, proper error matrix, and with $p_T > 200\text{ MeV}/c$ are accepted. The relaxed requirements on the soft-pion tracks increase the reconstructed Λ_b^{*0} candidates' yield by a factor of approximately 2.6.

To reduce the background, a kinematic fit is applied to the resulting Λ_b^0 , π_s^- , and π_s^+ candidates that constrains them to originate from a common point. The Λ_b^0 candidates are not constrained to the Λ_b^0 mass in this fit. Furthermore, since the bottom-baryon resonance originates and decays at the primary vertex, the soft-pion tracks are required to originate from the primary vertex by requiring an impact parameter significance $d_0(\pi_s^\pm)/\sigma_{d_0}$ smaller than 3 [11,12] determined by maximizing the quantity $S_{MC}/(1 + \sqrt{B})$.

The observed Q -value distribution is shown in Fig. 2. A narrow structure at $Q \approx 21\text{ MeV}/c^2$ is clearly seen. The projection of the corresponding unbinned likelihood fit is overlaid on the data. The fit function includes a signal and a smooth background. The signal is parametrized by two Gaussian functions with common mean, and widths and relative sizes set according to Monte Carlo simulation studies. Approximately 70% of the signal function is a narrow core with $0.9\text{ MeV}/c^2$ width, while the wider tail portion has a width of about $2.3\text{ MeV}/c^2$. The background is described by a second-order polynomial. The fit parameters

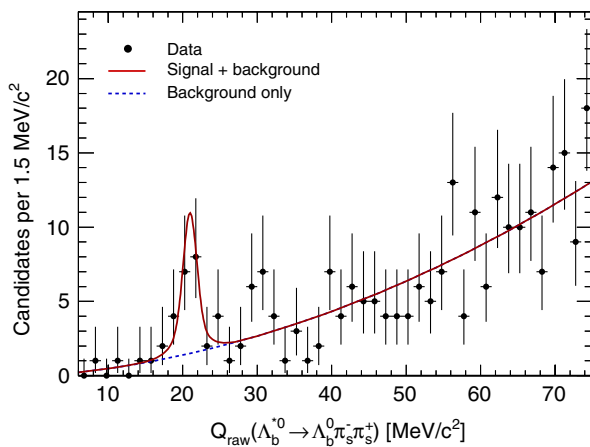


FIG. 2 (color online). Distribution of Q value for Λ_b^{*0} candidates, with fit projection overlaid.

are the position of the signal and its event yield. The negative logarithm of the extended likelihood function is minimized over the unbinned set of Q values observed. The fit over the Q range $6\text{--}75\text{ MeV}/c^2$ finds $17.3^{+5.3}_{-4.6}$ signal candidates at $Q = 20.96 \pm 0.35\text{ MeV}/c^2$.

The significance of the signal is determined using a log-likelihood-ratio statistic, $D = -2 \ln(\mathcal{L}_0/\mathcal{L}_1)$ [35,36]. We define the hypothesis \mathcal{H}_1 as corresponding to the presence of a Λ_b^{*0} signal in addition to the background and described by the likelihood \mathcal{L}_1 . The null hypothesis \mathcal{H}_0 assumes the presence of only background with a mass distribution described by the likelihood \mathcal{L}_0 and is nested in \mathcal{H}_1 . The \mathcal{H}_1 hypothesis involves two additional degrees of freedom with respect to \mathcal{H}_0 , the signal position, and its size. The significance for a Q search window of $6\text{--}45\text{ MeV}/c^2$ is determined by evaluating the distribution of the log-likelihood ratio in pseudoexperiments simulated under the \mathcal{H}_0 hypothesis. The fraction of the generated trials yielding a value of D larger than that observed in experimental data determines the significance. The fraction is 2.3×10^{-4} corresponding to a significance for the signal equivalent to 3.5 one-tailed Gaussian standard deviations.

The systematic uncertainties on the mass determination derive from the tracker momentum scale, the resolution model, and the choice of the background model. To calibrate the momentum scale, the energy loss in the tracker material and the intensity of the magnetic field must be determined. Both effects are calibrated and analyzed in detail using large samples of J/ψ , $\psi(2S)$, $Y(1S)$, and Z^0 particles reconstructed in the $\mu^+\mu^-$ decay modes as well as $D^{*+} \rightarrow D^0(\rightarrow K^-\pi^+)\pi^+$, and $\psi(2S) \rightarrow J/\psi(\rightarrow \mu^+\mu^-)\pi^+\pi^-$ samples [37,38]. The corresponding corrections are taken into account by the tracking algorithms. Any systematic uncertainties on these corrections are negligible in the Q -value measurements due to the mass difference term, $m(\Lambda_b^0 \pi_s^- \pi_s^+) - m(\Lambda_b^0)$. The uncertainties on the measured mass differences due to the momentum scale of the low- p_T π_s^\pm tracks are estimated from a large calibration sample of $D^{*+} \rightarrow D^0 \pi_s^+$ decays. A scale factor of 0.990 ± 0.001 for the soft-pion transverse momentum is found to correct the difference between the Q value observed in D^{*+} decays and its known value [3]. The same factor applied to the soft pions in a full simulation of $\Lambda_b^{*0} \rightarrow \Lambda_b^0 \pi_s^- \pi_s^+$ decays yields a Q -value change of $-0.28\text{ MeV}/c^2$. Taking the full value of the change as the uncertainty, we adjust the Q value determined by the fit to the Λ_b^{*0} candidates by $-0.28 \pm 0.28\text{ MeV}/c^2$. The Monte Carlo simulation underestimates the detector resolution, and the uncertainty of this mismatch is considered as another source of systematic uncertainty [12]. To evaluate the systematic uncertainty due to the resolution, we use a model with floating width parameter where only the ratio of the widths of the two Gaussians is fixed. The resulting uncertainty is found to be $\pm 0.11\text{ MeV}/c^2$. To estimate the

uncertainty associated with the choice of background shape, we increase the degree of the chosen polynomial and find the uncertainty to be $\pm 0.03 \text{ MeV}/c^2$. The statistical uncertainties on the resolution-model parameters due to the finite size of the simulated data sets introduce a negligible contribution. Adding in quadrature the uncertainties of all sources results in a total Q -value systematic uncertainty of $\pm 0.30 \text{ MeV}/c^2$.

Hence, the measured Q value of the identified Λ_b^{*0} state is found to be $20.68 \pm 0.35(\text{stat}) \pm 0.30(\text{syst}) \text{ MeV}/c^2$. Using the known values of the charged pion and Λ_b^0 baryon masses [3], we obtain the absolute Λ_b^{*0} mass value to be $5919.22 \pm 0.35(\text{stat}) \pm 0.30(\text{syst}) \pm 0.60(\Lambda_b^0) \text{ MeV}/c^2$, where the last uncertainty is the world's average Λ_b^0 mass uncertainty reported in Ref. [3]. The result is closest to the calculation based on $1/m_Q$, $1/N_c$ expansions [9]. The result is also consistent with the higher state $\Lambda_b^{*0}(5920)$ recently observed by the LHCb experiment [20]. LHCb also reports a state at approximately $5912 \text{ MeV}/c^2$ [20]. Assuming similar relative production rates and relative efficiencies for reconstructing the $\Lambda_b^{*0}(5912)$ and $\Lambda_b^{*0}(5920)$ states in the CDF II and LHCb detectors, the lack of a visible $\Lambda_b^{*0}(5912)$ signal in our data is statistically consistent within 2σ with the $\Lambda_b^{*0}(5912)$ yield reported by LHCb.

In conclusion, we conduct a search for the $\Lambda_b^{*0} \rightarrow \Lambda_b^0 \pi^- \pi^+$ resonance state in its Q -value spectrum. A narrow structure is identified at $5919.22 \pm 0.76 \text{ MeV}/c^2$ mass with a significance of 3.5σ . This signal is attributed to the orbital excitation of the bottom baryon Λ_b^0 and supports similar findings in proton-proton collisions.

We thank the Fermilab staff and the technical staffs of the participating institutions for their vital contributions. This work was supported by the U.S. Department of Energy and National Science Foundation; the Italian Istituto Nazionale di Fisica Nucleare; the Ministry of Education, Culture, Sports, Science and Technology of Japan; the Natural Sciences and Engineering Research Council of Canada; the National Science Council of the Republic of China; the Swiss National Science Foundation; the A. P. Sloan Foundation; the Bundesministerium für Bildung und Forschung, Germany; the Korean World Class University Program, the National Research Foundation of Korea; the Science and Technology Facilities Council and the Royal Society, UK; the Russian Foundation for Basic Research; the Ministerio de Ciencia e Innovación, and Programa Consolider-Ingenio 2010, Spain; the Slovak R&D Agency; the Academy of Finland; the Australian Research Council (ARC); the EU community Marie Curie Fellowship Contract No. 302103.

-
- [1] M. Neubert, *Phys. Rep.* **245**, 259 (1994); A. V. Manohar and M. B. Wise, *Heavy Quark Physics*, Cambridge Monographs on Particle Physics, Nuclear Physics and Cosmology, Vol. 10 (Cambridge University Press, Cambridge, England, 2000), p. 1.
 - [2] N. Isgur and M. B. Wise, *Phys. Lett. B* **232**, 113 (1989); **237**, 527 (1990); *Phys. Rev. D* **42**, 2388 (1990).
 - [3] J. Beringer *et al.* (Particle Data Group), *Phys. Rev. D* **86**, 010001 (2012) and 2013 partial update for the 2014 edition.
 - [4] J. G. Korner, M. Kramer, and D. Pirjol, *Prog. Part. Nucl. Phys.* **33**, 787 (1994).
 - [5] Throughout the text the notation Λ_b^{*0} represents the $J^P = \frac{1}{2}^-$ or the $J^P = \frac{3}{2}^-$ state.
 - [6] M. Karliner, B. Keren-Zur, H. J. Lipkin, and J. L. Rosner, *Ann. Phys. (Amsterdam)* **324**, 2 (2009); M. Karliner, *Nucl. Phys. B, Proc. Suppl.* **187**, 21 (2009).
 - [7] H. Garcilazo, J. Vijande, and A. Valcarce, *J. Phys. G* **34**, 961 (2007).
 - [8] D. Ebert, R. N. Faustov, and V. O. Galkin, *Phys. Rev. D* **72**, 034026 (2005); *Phys. Lett. B* **659**, 612 (2008); *Phys. At. Nucl.* **72**, 178 (2009).
 - [9] Z. Aziza Baccouche, C.-K. Chow, T. D. Cohen, and B. A. Gelman, *Phys. Lett. B* **514**, 346 (2001); *Nucl. Phys. A* **696**, 638 (2001).
 - [10] J. R. Zhang and M. Q. Huang, *Phys. Rev. D* **78**, 094015 (2008); *Chinese Phys. C* **33**, 1385 (2009).
 - [11] T. Aaltonen *et al.* (CDF Collaboration), *Phys. Rev. Lett.* **99**, 202001 (2007).
 - [12] T. Aaltonen *et al.* (CDF Collaboration), *Phys. Rev. D* **85**, 092011 (2012).
 - [13] V. M. Abazov *et al.* (D0 Collaboration), *Phys. Rev. Lett.* **99**, 052001 (2007).
 - [14] T. Aaltonen *et al.* (CDF Collaboration), *Phys. Rev. Lett.* **99**, 052002 (2007).
 - [15] T. Aaltonen *et al.* (CDF Collaboration), *Phys. Rev. D* **80**, 072003 (2009).
 - [16] V. M. Abazov *et al.* (D0 Collaboration), *Phys. Rev. Lett.* **101**, 232002 (2008).
 - [17] T. Aaltonen *et al.* (CDF Collaboration), *Phys. Rev. Lett.* **107**, 102001 (2011).
 - [18] R. Aaij *et al.* (LHCb Collaboration), *Phys. Rev. Lett.* **110**, 182001 (2013).
 - [19] S. Chatrchyan *et al.* (CMS Collaboration), *Phys. Rev. Lett.* **108**, 252002 (2012).
 - [20] R. Aaij *et al.* (LHCb Collaboration), *Phys. Rev. Lett.* **109**, 172003 (2012).
 - [21] D. Acosta *et al.* (CDF Collaboration), *Phys. Rev. D* **71**, 032001 (2005).
 - [22] T. Aaltonen *et al.* (CDF Collaboration), *Nucl. Instrum. Methods Phys. Res., Sect. A* **729**, 153 (2013).
 - [23] A. A. Affolder *et al.*, *Nucl. Instrum. Methods Phys. Res., Sect. A* **526**, 249 (2004).

- [24] We use a cylindrical coordinate system with z axis along the nominal proton beam line, radius r measured from the beam line, and ϕ defined as an azimuthal angle. The transverse plane (r, ϕ) is perpendicular to the z axis. The polar angle θ is measured from the z axis. Transverse momentum p_T is the component of the particle's momentum projected onto the transverse plane. Pseudorapidity is defined as $\eta \equiv -\ln(\tan(\theta/2))$. The impact parameter of a charged-particle track d_0 is defined as the distance of closest approach of the particle track to the point of origin (primary vertex) in the transverse plane.
- [25] E.J. Thomson *et al.*, *IEEE Trans. Nucl. Sci.* **49**, 1063 (2002).
- [26] B. Ashmanskas *et al.*, *Nucl. Instrum. Methods Phys. Res., Sect. A* **518**, 532 (2004); L. Ristori and G. Punzi, *Annu. Rev. Nucl. Part. Sci.* **60**, 595 (2010).
- [27] P. Nason, S. Dawson, and R.K. Ellis, *Nucl. Phys.* **B303**, 607 (1988); **B327**, 49 (1989).
- [28] C. Peterson, D. Schlatter, I. Schmitt, and P.M. Zerwas, *Phys. Rev. D* **27**, 105 (1983).
- [29] D.J. Lange, *Nucl. Instrum. Methods Phys. Res., Sect. A* **462**, 152 (2001).
- [30] R. Brun, R. Hagelberg, M. Hansroul, and J.C. Lassalle, CERN Reports No. CERN-DD-78-2-REV and No. CERN-DD-78-2.
- [31] All references to a specific charge combination imply the charge conjugate combination as well.
- [32] G. Punzi, in *Proceedings of the Conference on Statistical Problems in Particle Physics, Astrophysics and Cosmology, PHYSTAT 2003, Stanford, USA, 2003*, edited by L. Lyons, R.P. Mount, and R. Reitmeyer, eConf C030908, MODT002 (2003).
- [33] A. Abulencia *et al.* (CDF Collaboration), *Phys. Rev. Lett.* **98**, 122002 (2007).
- [34] T. Aaltonen *et al.* (CDF Collaboration), *Phys. Rev. Lett.* **104**, 102002 (2010).
- [35] S.S. Wilks, *Ann. Math. Stat.* **9**, 60 (1938).
- [36] R. Royall, *J. Am. Stat. Assoc.* **95**, 760 (2000).
- [37] D. Acosta *et al.* (CDF Collaboration), *Phys. Rev. Lett.* **96**, 202001 (2006).
- [38] T. Aaltonen *et al.* (CDF Collaboration), *Phys. Rev. Lett.* **103**, 152001 (2009).